AGU ADVANCING EARTH AND SPACE SCIENCES

Space Weather

RESEARCH ARTICLE
10.1029/2024SW004136

Special Collection:
Impact of Space Weather Events on Transportation System

Optimizing Polar Air Traffic: Strategies for Mitigating the Effects of Space Weather-Induced Communication Failures Poleward of 82°N

Dabin Xue[1,2,3], Zhizhao Liu[1], Donghe Zhang[4], Cheng-Lung Wu[3], and Jian Yang[2]

[1]Department of Land Surveying and Geo-Informatics, The Hong Kong Polytechnic University, Kowloon, China, [2]Department of Earth and Space Sciences, Southern University of Science and Technology, Shenzhen, China, [3]School of Aviation, University of New South Wales Sydney, Kensington, NSW, Australia, [4]School of Earth and Space Sciences, Peking University, Beijing, China

Key Points:

- Simulations are conducted to explore the impact of space weather-caused communication failures on polar flights
- Air traffic management strategies are proposed in response to communication failures north of 82°
- Economic losses from communication failures on polar flights are estimated according to different air traffic management strategies

Correspondence to:
Z. Liu and J. Yang,
lszzliu@polyu.edu.hk;
yangj36@sustech.edu.cn

Citation:
Xue, D., Liu, Z., Zhang, D., Wu, C.-L., & Yang, J. (2024). Optimizing polar air traffic: Strategies for mitigating the effects of space weather-induced communication failures poleward of 82°N. *Space Weather*, *22*, e2024SW004136. https://doi.org/10.1029/2024SW004136

Received 27 AUG 2024
Accepted 31 OCT 2024

Author Contributions:
Conceptualization: Dabin Xue, Cheng-Lung Wu, Jian Yang
Formal analysis: Dabin Xue, Zhizhao Liu, Donghe Zhang, Cheng-Lung Wu
Funding acquisition: Zhizhao Liu
Investigation: Zhizhao Liu, Donghe Zhang, Cheng-Lung Wu, Jian Yang
Methodology: Dabin Xue, Cheng-Lung Wu
Supervision: Zhizhao Liu, Jian Yang
Validation: Dabin Xue, Donghe Zhang, Cheng-Lung Wu, Jian Yang
Visualization: Donghe Zhang
Writing – original draft: Dabin Xue

Abstract Aviation communication is significant for the safe, efficient, and orderly operation of air traffic. The aviation industry relies on a sophisticated network to maintain air-ground communications. However, space weather events can disrupt the ionosphere conditions and damage satellites, leading to High-Frequency (HF) communication blackouts and satellite communication failures. These disruptions can jeopardize flight safety, especially for flights over polar regions. In response, strategies such as cancellations, rescheduling, or rerouting to lower latitudes may be necessary, despite the low flight efficiency and substantial financial losses. With the background of the anticipated solar maximum in 2025 and a growing number of polar flights, it is indispensable to have a comprehensive understanding of the space weather effects on aviation communication and develop constructive strategies from an Air Traffic Management (ATM) perspective. Hence, we simulate scenarios with different durations of communication failures and assess the corresponding economic losses. Based on the data derived from historical polar flights in 2019, there are daily 18 polar flights with trajectories crossing the north polar region higher than 82°N. Simulation results show that the economic losses associated with these polar flights can range from €0.03 million to €1.32 million, depending on both the duration of communication failures and the adopted air traffic management strategies. We believe that this study can shed light on the effects of space weather-induced communication failures on polar flight operations and provide guidance for mitigating these effects in the aviation industry.

Plain Language Summary Effective communication is compulsory in aviation operations, with Very High Frequency (VHF) being the primary mode of communication between aircraft and ground stations. High Frequency (HF) communication and satellite communications come into play when aircraft traverse in the north polar region higher than 82°N. However, both forms of communication may experience failures due to changes in ionospheric conditions and degraded satellite performances caused by space weather. As a result, the routine operations of polar flights will be disrupted. To mitigate this, we propose targeted Air Traffic Management (ATM) strategies such as flight cancellations, rescheduling, and rerouting. In 2019, an average of 18 polar flights per day crossed the North Polar region at latitudes exceeding 82°N. Based on simulations of communication failure durations, the economic losses associated with these polar flights would vary from €0.03 million to €1.32 million. We hope this study can be a foundational reference for the aviation industry making decisions in response to communication failures caused by space weather.

1. Introduction

Effective communication in aviation plays a pivotal role in ensuring the safe and efficient operation of flights (Alharasees et al., 2023). Pilots rely on communication with ground stations to receive crucial instructions, weather condition updates, and nearby air traffic information (Bain et al., 2023; Xue et al., 2021). The Very High Frequency (VHF, 30–300 MHz) is the primary channel used for communication between pilots and aviation staff at ground stations. Specifically, pilots employ the Aircraft Communications Addressing and Reporting System (ACARS, 131.550 MHz) to communicate with airline dispatchers (Smith et al., 2018). Additionally, the Controller Pilot Data Link Communication (CPDLC, 118.000–136.975 MHz) facilitates communication between pilots and Air Traffic Control Officers (ATCOs) (Lin et al., 2012). Nevertheless, polar flights typically do not rely on VHF communication for the entire duration of the flight, as VHF is limited to line-of-sight communication between aircraft and ground stations, effective only within a short range of about 160 km (Pinkerton, 2019). In

Writing – review & editing: Zhizhao Liu, Donghe Zhang, Jian Yang

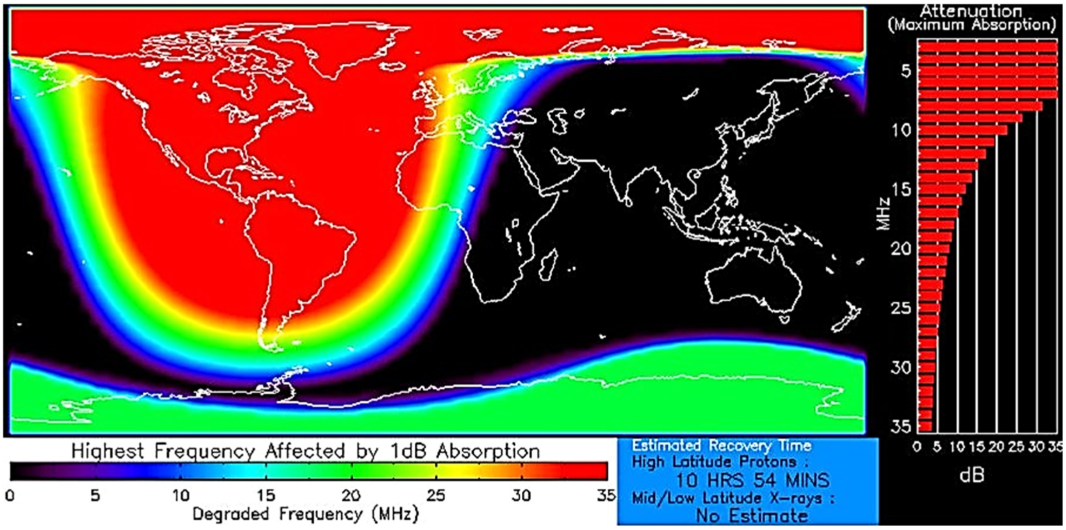

Figure 1. PCA due to SEPs accelerated by solar flares of the sunspot AR3664 (https://www.spaceweather.com/).

polar regions, the remoteness and Earth's curvature hinder reliable VHF communication over such long distances (Tooley & Wyatt, 2017). Instead, polar flights utilize alternative methods such as High Frequency (HF, 3–30 MHz) radios and Satellite Communication (SATCOM). Notably, when flights traverse areas north of 82°N, where geostationary satellite communications are unavailable due to the satellites' orbit inclination, aircraft can only use HF radios or polar satellite communication systems like Iridium to maintain a dependable connection with ground stations (Anderson et al., 2021; Chen et al., 2021). With the rapid advancement of low Earth orbit (LEO) satellite technologies, emerging SpaceX Starlink (McDowell, 2020) and OneWeb (Li et al., 2021) offer a promising solution for providing continuous, global connectivity to aircraft (Caspi et al., 2022; Ma et al., 2023). However, to the best of our knowledge, there are no comprehensive studies specifically investigating the use of these two ultra-dense LEO networks for pilot communication or navigation.

HF communication relies on the ionosphere to transmit signals over long distances (Ruck & Themens, 2021). The ionosphere, a region of the Earth's upper atmosphere, contains charged particles that can reflect and refract HF radio signals. This property allows HF signals to bounce off the ionosphere and travel beyond the horizon, making it particularly suitable for long-range communication (Bust et al., 2021). However, HF communication in the Arctic region may be hindered by Polar Cap Absorption (PCA) events, which occur when Solar Energetic Particles (SEPs) ionize the polar D-region ionosphere. These particles, primarily with energies between 1 and 100 MeV, can reach Earth within tens of minutes to a few hours after their emission, depending on their energy (Hapgood et al., 2021). While the geomagnetic field shields the SEPs from entering the lower and mid-latitudes, the SEPs precipitate into the entire polar cap ionosphere, enhancing D-region ionization and leading to significant HF radio absorption (Tsurutani et al., 2009, 2022). In contrast, Extreme Ultra-Violet (EUV) and X-ray emissions from solar flares can significantly enhance the ionospheric Total Electron Content (TEC) in the dayside, particularly near Earth's subsolar point, but the TEC increase in regions above 82°N is slight (Tsurutani et al., 2005). Coronal Mass Ejections (CMEs) that accompany intense solar flares take one to 4 days to reach Earth and trigger magnetic storms only if their magnetic fields are southward-directed (Echer et al., 2008; Tsurutani et al., 2022). For example, protons accelerated by solar flares in the magnetic canopy of AR3664 traveled along the Parker Spiral back to Earth on 14 May 2024. These particles were channeled by the Earth's magnetic field toward the poles, where they ionized the atmosphere and disrupted normal shortwave radio transmissions. The red zones in Figure 1 indicate areas where shortwave radio signals were being absorbed. Within the Arctic Circle, radio frequencies below 30 MHz are largely inaccessible, posing significant challenges for polar aviators who rely on the HF bands.

As another aviation communication method in polar regions, SATCOM provides reliable communication by utilizing polar satellites. This method ensures continuous communication even in the most remote areas where VHF and HF might be less effective. While mega constellations are designed to enhance coverage and redundancy (Long & Zhang, 2024; Zhang et al., 2022), marking a significant shift in SATCOM systems, individual

Table 1
Aviation Communication Conditions for Polar Flights Operating South and North of 82°N

	South of 82°N	North of 82°N		
Condition #	SATCOM[1]	HF	SATCOM[2]	Operation status
1	×	√	√	Canceled
2	×	√	×	Canceled
3	×	×	√	Canceled
4	×	×	×	Canceled
5	√	√	√	Normal
6	√	√	×	Normal
7	√	×	√	Normal
8	√	×	×	?

Note. SATCOM[1] refers to satellite communication using geostationary or polar satellites, while SATCOM[2] refers specifically to communication using polar satellites. Label '×' indicates communication failures, while label '√' signifies normal communications.

satellites within these constellations may still experience signal degradation during space weather events. First, as an electromagnetic wave-based communication system, SATCOM is influenced by changes in ionospheric conditions (Goodman, 2005). Sudden and unpredictable alterations in the ionosphere can induce ionospheric scintillation, a phenomenon characterized by fluctuations in signal amplitude, phase, and arrival angle, potentially degrading communication quality and, in extreme cases, causing disruptions (Portella et al., 2021; Song et al., 2020). Second, space weather events like solar storms unleash vast amounts of high-energy charged particles that can interfere with satellite operations, potentially causing malfunctions or even direct damage to onboard electronic equipment and components (Horne et al., 2013; Singh et al., 2010). Lastly, increased thermospheric drag during space weather events can threaten satellite performance (Oliveira & Zesta, 2019), particularly in polar and high-latitude regions (Kleimenova et al., 2021).

Solar activity follows an 11-year cycle and now it is in the 25th solar cycle with the solar maximum around 2025 (Hapgood et al., 2022; Okoh et al., 2018). It is foreseeable that space weather will impact flight operations in the near future. Despite the provision of space weather advisories for the aviation industry, it remains crucial to propose corresponding strategies from the perspective of Air Traffic Management (ATM) to mitigate the adverse effects of upcoming space weather events. The effects of satellite navigation failure on flight operations and the associated economic losses have been assessed (Xue et al., 2022a, 2023a). Furthermore, in response to increased cosmic radiation, Xue, Yang, Liu, et al. (2022) proposed a multi-objective model by assigning optimal flight altitudes and speeds to reduce fuel consumption and aviation radiation exposure. Moreover, based on the assumption that a space weather event as intense as the 2003 Halloween solar storm would have occurred in 2019, the economic losses incurred in global aviation operations had been quantified. If all polar flights were canceled for an entire day, the direct economic loss was estimated to be about 2.20 million Euros (Xue, Yang, Liu, & Yu, 2023; Zinke, 2023).

Despite the significance, research on the effects of space weather on flight operations remains limited. Table 1 outlines the aviation communication conditions for polar flights operating south and north of 82°N. Under conditions #1–4, polar flights must be canceled. Conditions #5–7 allow for normal operations of polar flights. However, targeted ATM solutions are necessary under condition #8 to mitigate the effects of communication failures north of 82°N. This study specifically addresses condition #8, in which space weather events cause both HF communication blackouts and SATCOM failures north of 82°N. To address this problem and alleviate the negative consequences of communication failures in this area, we propose corresponding strategies from the perspective of air traffic management. Using polar flight data from 2019, we estimate the potential economic losses under various simulated scenarios. This study is expected to serve as a guideline for decision-making within the aviation industry in response to space weather-caused communication failures in the polar region.

2. Polar Flight Data

Polar routes, aptly named for the trajectory over the Earth's poles, are defined by the Federal Aviation Administration (FAA) as the North Polar area, encompassing regions north of 78°N (FAA, 2022). This includes the Arctic Ocean, as well as the northern areas of Europe, Asia, and North America. Typically, north polar routes, adopted for flights between Asian and North American cities, offer a more efficient routing, which reduces flight times, fuel consumption, and emissions. According to (NAV CANADA, 2017), a flight from New York to Hong Kong can save up to two hours of flying time and 16,000 L of fuel by using polar routes. Over the years, there was a significant surge in air traffic operating on polar routes, experiencing a 15-fold increase between 2003 and 2015. In 2016 alone, more than 14,000 flights utilized these polar routes. In particular, polar routes passing through Canadian airspace are estimated to result in an annual reduction of over 600,000 tons of greenhouse gas emissions (NAV CANADA, 2017). While the North Pole experiences significant air traffic growth, the South Pole lacks a comparable level of air traffic. This can be attributed to the harsher weather conditions, a limited number of diversion airports, and the lower population density in the southern hemisphere. At present, no airline operates a

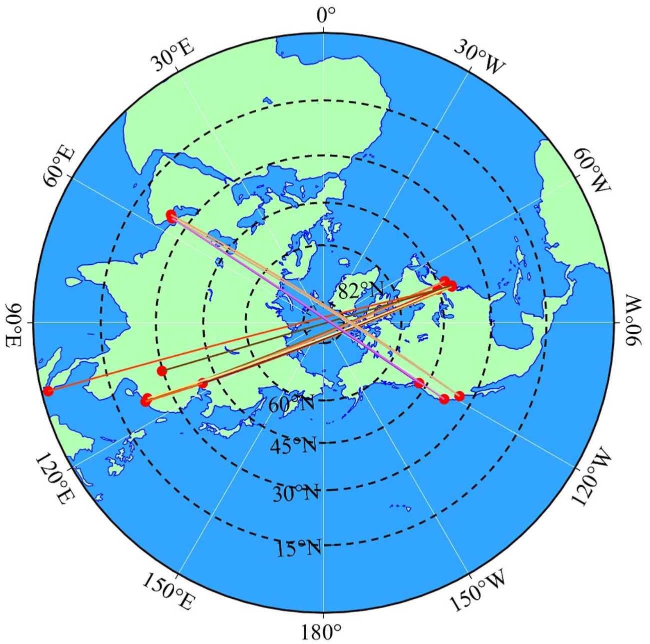

Figure 2. Flight paths of polar flights with GCR traversing the area north of 82°N. Airports are denoted as red dots.

south polar route, but certain flight routes between Australia and South America and between Australia and South Africa skirt the Antarctic coastline.

As aircraft can only use HF communication and polar satellite-based SATCOM in the area north of 82°N to communicate with ground stations, our attention is directed solely to these polar flights with Great Circle Routes (GCR) traversing the area north of 82°N. To investigate the effects of communication failures on polar flights, we conducted a simulated case study using flight data from 6 April 2019 (UT), which included 18 polar flights passing through the area north of 82°N. Please note that no space weather event occurred on this day. Additionally, we acknowledge that polar flights experience seasonal variations primarily driven by passenger demand, such as tourism and business travel (Merkert & Webber, 2018; Wang et al., 2023). Airlines typically adjust their schedules to meet higher demand during the summer months, holidays, and major events. As a result, the outcomes of this study may differ from real-world operations, as the final results are influenced by the number of polar flights. Figure 2 illustrates the GCR, and Table 2 provides detailed information on these polar flights, including flight callsign, aircraft type, departure and destination cities, etc. In this simulation, it is assumed that the flight plans on other days are the same as those on 6 April 2019, although the number of polar flights may vary due to various factors, such as airline decisions, global events, and seasonal considerations.

3. ATM Strategy for Communication Failures Poleward of 82°N

To alleviate the effects of space weather on aviation, four space weather centers have been established to monitor and forecast space weather events (Hapgood, 2022). These four Space Weather Centers (SWXCs) are (a) the Pan-European Consortium for Aviation Space Weather User Services (PECASUS), comprising Finland, Belgium, the United Kingdom, Austria, Germany, Italy, Netherlands, Poland, Cyprus, and South Africa; (b) the National Oceanic and Atmospheric Administration (NOAA) Space Weather Prediction Center (SWPC); (c) the consortium of Australia, Canada, France, and Japan (ACFJ); and (d) the China-Russia Consortium (CRC) (Kauristie et al., 2021). These centers operate on a rotational basis, with one serving as the on-duty center and the others as the primary and secondary backup centers and the maintenance center, each monitoring space weather conditions in a 2-week shift.

The International Civil Aviation Organization (ICAO) mandates continuous and effective communication for aircraft throughout their entire flight paths (ICAO, 2008). Considering that there are ∼2,000 radio blackouts due to solar activity during each 11-year solar cycle (Dobrijevic, 2022), relying solely on space weather forecast advisories is insufficient. Therefore, it is necessary to propose strategies for both airborne flights (already taken off) and flights on the ground (not taking off yet) from the standpoint of air traffic management. Figure 3a provides a schematic diagram illustrating the process of space weather monitoring and the subsequent ATM strategies. The procedures are detailed as follows.

1. Space weather centers collect data from diverse sources, including ground-based observatories, satellites, and solar-monitoring instruments. This data set comprises details about solar activity, solar wind, magnetic fields, and other pertinent parameters. Furthermore, ongoing observations of the Sun are conducted to monitor solar flares, coronal mass ejections, sunspots, and other solar phenomena. Instruments like solar telescopes and satellites are utilized to provide real-time data (Darnel et al., 2022; Palmerio et al., 2022).
2. Space weather centers analyze the collected data to identify patterns, trends, and potential space weather events. Advanced algorithms and models are utilized to process and interpret the vast amount of information (Chen et al., 2022; Kay et al., 2022; Kruglyakov et al., 2022).
3. Based on the analysis, space weather centers produce space weather advisories related to HF communications and SATCOM, as presented in Figure 3b. Please note that SATCOM has been identified as the fourth impact area. However, advisories for SATCOM will not be issued until further work is conducted to develop and validate operationally relevant advisory thresholds (Bureau of Meteorology, 2023).

Table 2
Information About 18 North Polar Flights With GCR Traversing the Area North of 82°N, Ordered by the Commencement Time of Their Traversing Over 82°N

Flight index	Flight callsign	Aircraft type	Seat capacity	Indirect cancellation cost (€)	Polar flight route (departure-destination)	Flight time (DD HH: MM)	Duration over 82°N (DD HH: MM)	(min)
01	CCA880	B789	252	40,156	Montréal-Beijing	05 19:23-06 09:38	06 01:14-06 02:58	104
02	CHH482	B789	252	40,156	Boston-Beijing	05 21:13-06 09:32	06 02:23-06 04:05	102
03	UAE230	B773	360	49,120	Seattle-Dubai	06 00:11-06 13:54	06 04:37-06 06:37	120
04	UAE226	A388	469	58,167	San Francisco-Dubai	06 00:32-06 15:21	06 06:11-06 08:08	117
05	ETD170	B773	360	49,120	Los Angeles-Abu Dhabi	06 00:19-06 15:48	06 06:48-06 08:06	78
06	UAE216	A388	469	58,167	Los Angeles-Dubai	06 00:29-06 15:43	06 06:49-06 08:17	88
07	CPA811	B773	360	49,120	Boston-Hong Kong	06 06:00-06 21:06	06 11:19-06 13:09	110
08	CPA899	A359	293	43,559	Newark-Hong Kong	06 05:50-06 21:00	06 11:35-06 12:50	75
09	CPA845	B773	360	49,120	New York-Hong Kong	06 05:51-06 21:09	06 11:36-06 12:58	82
10	CHH416	B789	252	40,156	New York-Chongqing	06 07:07-06 21:05	06 12:24-06 14:25	121
11	CCA990	B773	360	49,120	New York-Beijing	06 06:37-06 19:50	06 12:30-06 13:53	83
12	ETD171	B773	360	49,120	Abu Dhabi-Los Angeles	06 05:11-06 21:14	06 13:10-06 14:31	81
13	UAE225	A388	469	58,167	Dubai-San Francisco	06 06:21-06 21:41	06 13:49-06 15:50	121
14	UAE215	A388	469	58,167	Dubai-Los Angeles	06 06:15-06 21:51	06 13:52-06 15:22	90
15	UAE229	B773	360	49,120	Dubai-Seattle	06 06:33-06 20:35	06 14:00-06 16:02	122
16	SIA21	A359	293	43,559	Newark-Singapore	06 15:29-07 08:25	06 20:36-06 22:28	112
17	CSN300	B773	360	49,120	New York-Guangzhou	06 16:23-07 06:05	06 21:31-06 22:53	82
18	UAL89	B772	336	47,128	Newark-Beijing	06 16:10-07 04:57	06 21:53-06 23:09	76

Note. The indirect cancellation costs are sourced from (Eurocontrol, 2020).

4. After receiving the alerts and warnings, the aviation industry, including airports, airlines, and Air Traffic Control (ATC), would conduct Collaborative Decision Making (CDM) by considering all stakeholder needs before making decisions (Albers & Rundshagen, 2020; Di Vaio & Varriale, 2020). The contribution of this study is to mitigate the effects of space weather-induced communication failures north of 82°N on polar flight operations by providing practical and constructive strategies from the perspective of ATM.

3.1. Flight Emergency Diversion Due To Unpredicted Communication Failures

Due to the lack of accurate and timely space weather forecast information, flights may occasionally need to divert and land at alternate airports near the Arctic region, as illustrated in Figure 3c, including BGTL (76.53°N,

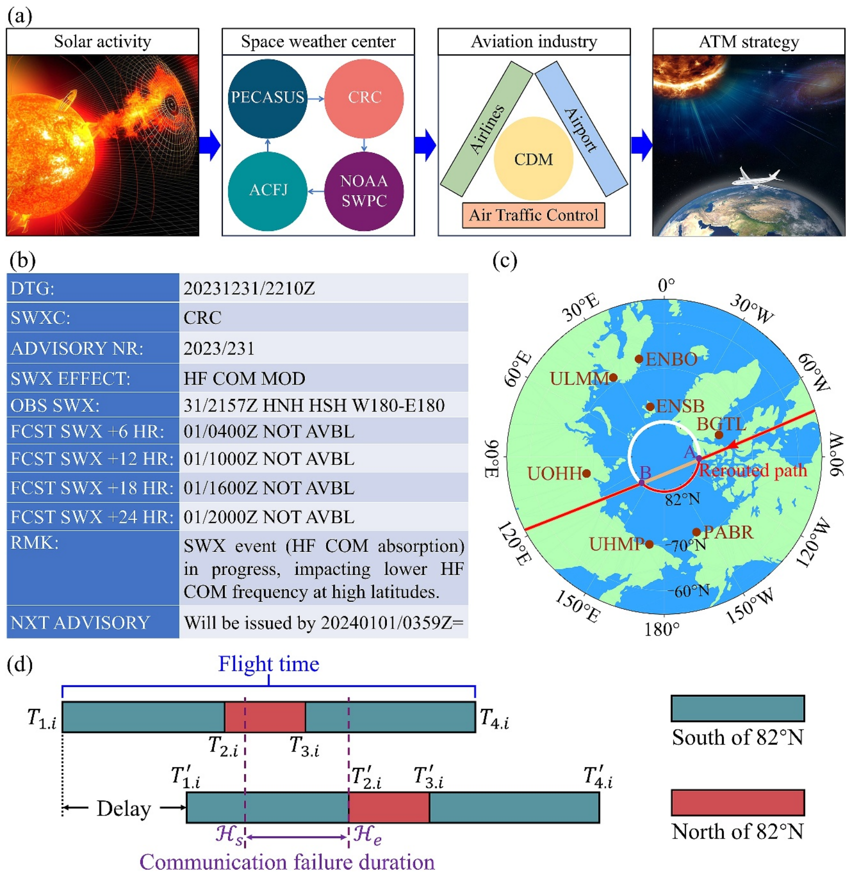

Figure 3. (a) The schematic diagram of space weather monitoring and subsequent aviation industry response; (b) An example of space weather advisory for HF communications; (c) Alternate airports near the Arctic region and flight rerouting methods for detouring the polar circle of 82°N; (d) Flight rescheduling to avoid the period of communication failures north of 82°N.

68.70°W), PABR (71.28°N, 156.77°W), UHMP (69.78°N, 170.60°E), UOHH (71.98°N, 102.50°E), ULMM (68.78°N, 32.75°E), ENBO (67.27°N, 14.37°E), and ENSB (78.25°N, 15.47°E) (Albright, 2020).

Flight diversion can disrupt airline operations, leading to changes in crew schedules and aircraft rotations (Malandri et al., 2020). This may have a cascading effect on subsequent flights and the overall efficiency of the airline's operation. In addition, diverting flights incurs additional costs for the airline, including expenses related to landing fees at the alternate airport, and fuel for the diversion. Besides, passengers on diverted flights may experience inconvenience, including delays, longer travel times, and potential challenges in connecting to subsequent flights (Hu et al., 2015). Moreover, flight diversion may lead to increased fuel consumption and emissions, especially if alternate airports are far away from their original destinations. Diversion costs estimated by EUROCONTROL vary from €6,000 to €68,500 (Eurocontrol, 2020). Alternatively, flights may reroute to the low-latitude region south of 82°N, if loaded fuel is sufficient. Details about rerouting can refer to Section 3.3.

3.2. Flight Cancellation

The most straightforward approach to tackle the issue of communication failures north of 82°N is to cancel the flights. In this case, if there are any periods of overlap between the durations of communication failures and the durations of polar flights traveling poleward of 82°N, the specific flights will be canceled. However, this method is consistently associated with several drawbacks. Airline revenue faces significant impact due to flight cancellations, including losses from ticket cancellations and potential expenses related to passenger compensations, rebooking, and operational adjustments. The disruption of airline operations, affecting crew schedules, aircraft utilization, and overall logistics, creates a cascading effect across the entire air transportation network. Passengers on canceled polar flights may encounter inconvenience, necessitating rescheduling or seeking alternative routes (Yimga & Gorjidooz, 2019).

3.3. Flight Rerouting

When space weather advisories predict there will be communication failures north of 82°N, polar flights can also choose to reroute to low-latitude regions to keep the line of sight with communication satellites. However, the new flight path may result in increased fuel consumption and emissions, particularly if the alternative route is longer or less fuel-efficient, contributing to the environmental impact of air travel (Xue et al., 2020). Besides, rerouting incurs additional costs for airlines, including expenses related to fuel for the extended route, potential fees for using different airspaces, and adjustments in crew and ground services (Chang, 2020). Additionally, the process of rerouting flights may necessitate adherence to diverse airspace regulations. Airlines are required to collaborate with pertinent aviation authorities to guarantee conformity with these regulations.

The original flight trajectory follows the GCR through points A and B, with the distance represented as $\overline{\mathrm{AB}}$, as illustrated in Figure 3c. Herein, a rerouting method is adopted along the 82°N polar circle, with the distance denoted as $\breve{\mathrm{AB}}$. This newly designed route results in a longer flight distance ($\breve{\mathrm{AB}} - \overline{\mathrm{AB}}$), leading to more fuel consumption and longer flight time. Appendix A provides the calculation methods for fuel consumption and flight time.

3.4. Flight Rescheduling

In anticipation of communication failures north of 82°N forecasted by space weather advisories, an alternative approach is to reschedule the flights. For each polar flight i, the original departure time and landing time are represented as $T_{1.i}$ and $T_{4.i}$, respectively. The original times of flight i entering and exiting the region north of 82°N are denoted as $T_{2.i}$ and $T_{3.i}$. The duration of communication failures is denoted as $\mathcal{H}$, with the start time and end times indicated as $\mathcal{H}_s$ and $\mathcal{H}_e$. If there is an overlap between the intervals $[T_{2.i},\ T_{3.i}]$ and $[\mathcal{H}_s, \mathcal{H}_e]$, that is, $[T_{2.i},\ T_{3.i}] \cap [\mathcal{H}_s, \mathcal{H}_e] \neq \varnothing$, it means that polar flight i will encounter communication failures during the original schedule. Hence, flight rescheduling is necessary to solve this problem. As shown in Figure 3d, the rescheduled times of departure time, landing time, entering and exiting the region north of 82°N are denoted by $T'_{1.i}$, $T'_{4.i}$, $T'_{2.i}$, and $T'_{3.i}$, respectively. Notably, $T'_{2.i}$ is equal to $\mathcal{H}_e$, allowing the calculation of ground delay time through the formula $D_i = T'_{2.i} - T_{2.i}$. In practical terms, certain airlines may establish a maximum delay time (Ψ), and if the projected ground delay surpasses this threshold, this flight would be canceled.

However, predicting the exact duration of communication failure caused by space weather is highly uncertain in real-world operation, making flight rescheduling a complex decision for airlines. The unpredictability of space weather necessitates a probabilistic approach to managing communication failure, particularly in polar regions. Airlines rely on probabilistic forecasts to assess risks, balancing operational efficiency with passenger safety when deciding whether to reroute flights or proceed with contingency plans. Current challenges include limited real-time data and low-resolution space weather models, leading to difficult decisions with potential cost and safety implications. To improve resilience, advancements are needed in higher-resolution forecasting, real-time data integration, and automated decision-support tools that help airlines make informed decisions in dynamic conditions. Collaborative efforts in space weather research are essential to enhance aviation's ability to manage these risks effectively.

4. Scenario Simulation

Space weather advisories are labeled by MOD and SEV based on various event parameters, which implies the impacts on HF communications might be severe. These event parameters include auroral absorption (Kp = 8, MOD; Kp = 9, SEV), Polar Cap Absorption (PCA) (riometer absorption ≥ 2 dB, MOD; riometer absorption ≥ 5 dB, SEV), shortwave fadeout (solar X-rays ≥ 10^{-4} W/m^2 (X1), MOD; solar X-rays ≥ 10^{-3} W/m^2 (X10), SEV), and Post Storm maximum useable frequency Depression (PSD) (MUF ≥ 30%, MOD; MUF ≥ 50%, SEV). According to (Fiori et al., 2022), for each solar cycle, there are.

1. 40 moderate auroral absorption events with a mean duration of 5.1 hr
2. 3 severe auroral absorption events with a mean duration of 12 hr
3. 24 moderate PCA events with a mean duration of 8 hr

4. 13 severe PCA events with a mean duration of 1.6 days
5. 123 moderate shortwave fadeout events with a mean duration of 68 min
6. 5 severe shortwave fadeout events with a mean duration of 132 min
7. 200 moderate PSD events with a mean duration of 5.5 hr
8. 56 severe PSD events with a mean duration of 8.5 hr

However, it is worth noting that only PCA events are the main ones affecting HF communications poleward of 82°N. In addition, space weather can also cause SATCOM failures by altering ionospheric conditions or damaging satellites (Knipp et al., 2016; Singh et al., 2021). Hence, to comprehensively explore the potential effects of communication failures poleward of 82°N on polar flights, five scenarios with durations of 1 hr, 6 hr, 12 hr, 24 hr, and 36 hr are simulated, all commencing at 00:00 UT. Specifically, S1: 00:00-01:00 UT, affecting 0 flight; S2: 00:00-06:00 UT, affecting 3 flights (flight index: 01–03); S3: 00:00-12:00 UT, affecting 9 flights (flight index: 01–09); S4: 00:00-00:00 (+1 day) UT, affecting 18 flights (flight index: 01–18); S5: 00:00-12:00 (+1 day) UT, affecting 27 flights (flight index: 01–18 and 01–09).

5. Result Analysis

After the scenario simulation of communication failures, this section explores the impact on polar flights and quantifies the associated economic losses. It is important to emphasize that simulation results are based on space weather advisory forecasts, specifically targeting polar flights that have not yet taken off. Hence, results about flight emergency diversion due to unpredicted space weather are not presented in this study. Instead, results about flight cancellation, rerouting, and rescheduling in various scenarios are presented in Sections 5.1, 5.2, and 5.3. Under S1 (00:00-01:00 UT), polar flights will not be affected as no flights cross the area north of 82°N during this short time interval.

5.1. Flight Cancellation Results

If flight cancellations are adopted as a response to communication failures poleward of 82°N, the number of canceled flights according to the proposed criterion in Section 3.2 is as follows: 3 (1 × B773 and 2×B789) under S2, 9 (1 × A359, 2 × A388, 4 × B773, and 2 × B789) under S3, 18 (2 × A359, 4 × A388, 1 × B772, 8 × B773, and 3 × B789) under S4, and 27 (3 × A359, 6 × A388, 1 × B772, 12 × B773, and 5 × B789) under S5. It is noteworthy that space weather events are uncontrollable, and airlines are not obliged to compensate passengers (U.S. Department of Transportation, 2022). However, other costs caused by the cancellation are inevitable, such as loss of revenue, interlining costs, loss of future value, crew and catering costs, luggage delivery costs, etc. According to (Eurocontrol, 2020), the indirect economic costs due to flight cancellation of each type of aircraft are estimated as €43,559 for A359 (293 seats), €58,167 for A388 (469 seats), €47,128 for B772 (336 seats), €49,120 for B773 (360 seats), and €40,156 for B789 (252 seats), which is also listed in Table 2. With such, the associated economic costs for the cancellation of flights under simulation scenarios S2, S3, S4, and S5 are €0.13 million, €0.44 million, €0.88 million, and €1.32 million, respectively.

5.2. Flight Rerouting Results

In Figure 3c, the aircraft is shown to reroute to fly along the polar circle at the latitude of 82°N. In practical applications, airlines can choose different polar circles (ϑ) based on specific regulations. Here, we select ϑ as 82°N and 75°N as two representative polar circles to evaluate the outcome of flight rerouting, with the results presented in Table 3. The average flight distance of all 18 polar flights is 12,570 km. Flight rerouting leads to an increase in flight distance, duration, and fuel consumption. For instance, the average flight distance increases by 338 km, constituting 2.69% of 12,570 km, if airlines choose the polar circle $\vartheta = 82°$N. In contrast, the average flight distance for $\vartheta = 75°$N experiences a larger increase, accounting for 8.62% of the total average flight distance. The average results for $\vartheta = 75°$N are three times as many as those for $\vartheta = 82°$N. Utilizing cruise speed data, the average increased flight time is calculated as 24 min for $\vartheta = 82°$N and 75 min for $\vartheta = 75°$N. According to Appendix A, the increased fuel consumption averages 3.3 tons for $\vartheta = 82°$N and 10.6 tons for $\vartheta = 75°$N.

Under different scenarios of simulating different durations of communication failures poleward of 82°N, the increased economic costs are evaluated by considering time-related costs (passenger time costs and airborne delay costs for airlines) and fuel costs. The longer flight time has an average cost of €74/min (Eurocontrol, 2020). Calculated based on an average passenger time value of €47/hour (Airlines for America, 2023) and an 80% seat

Table 3
Flight Rerouting Results Based on Different Latitudes of Rerouting Polar Circles ($\vartheta = 82°N$ and $\vartheta = 75°N$)

Flight index	Callsign	Duration over 82°N $\mathcal{H}$	Cruise altitude (m)	Cruise speed (knot)	Flight distance L (km)	$\vartheta = 82°N$ D (km)	T (min)	F (ton)	$\vartheta = 75°N$ D (km)	T (min)	F (ton)
01	CCA880	01:14-02:58	11,600	470	10,459	150	10	0.9	855	59	5.4
02	CHH482	02:23-04:05	11,600	480	10,828	281	19	1.8	1,042	70	6.5
03	UAE230	04:37-06:37	11,300	450	11,941	707	51	6.5	1,541	111	14.1
04	UAE226	06:11-08:08	11,600	460	13,034	648	46	10.1	1,478	104	23.0
05	ETD170	06:48-08:06	11,300	470	13,498	98	7	0.9	770	53	6.9
06	UAE216	06:49-08:17	11,600	460	13,415	160	11	2.5	872	61	13.6
07	CPA811	11:19-13:09	11,600	470	12,820	357	25	3.2	1,140	79	10.2
08	CPA899	11:35-12:50	12,200	470	12,974	82	6	0.6	742	51	5.1
09	CPA845	11:36-12:58	11,600	450	12,985	105	8	1.0	783	56	7.2
10	CHH416	12:24-14:25	11,300	470	12,205	942	65	6.0	1,781	123	11.3
11	CCA990	12:30-13:53	11,600	470	10,991	103	7	0.9	779	54	7.0
12	ETD171	13:10-14:31	11,600	470	13,498	98	7	0.9	770	53	6.9
13	UAE225	13:49-15:50	11,900	470	13,034	648	45	9.9	1,478	102	22.7
14	UAE215	13:52-15:22	11,900	470	13,415	160	11	2.5	872	60	13.4
15	UAE229	14:00-16:02	11,300	450	11,941	707	51	6.5	1,541	111	14.1
16	SIA21	20:36-22:28	12,200	480	15,353	602	41	4.2	1,428	96	9.8
17	CSN300	21:31-22:53	11,600	470	12,895	157	11	1.4	867	60	7.7
18	UAL89	21:53-23:09	11,900	470	10,980	85	6	0.6	749	52	5.4
Average:					**12,570**	**338**	**24**	**3.3**	**1,083**	**75**	**10.6**

Note. $\mathcal{H}$: Expected Duration Over 82°N; L: Original Distance of Great Circle Route; D: Increased Flight Distance; T: Increased Flight Time; F: NoteIncreased Fuel Consumption

occupancy factor, the unit time costs for all passengers due to flight delays are estimated as €184/min (A359, 293 seats), €294/min (A388, 469 seats), €211/min (B772, 336 seats), €226/min (B773, 360 seats), and €158/min (B789, 252 seats). In addition, fuel cost is another important expense for airlines. With the fuel price of €843/ton (IATA, 2024), Figure 4 shows the results of increased fuel costs for both $\vartheta = 82°N$ and $\vartheta = 75°N$ based on the

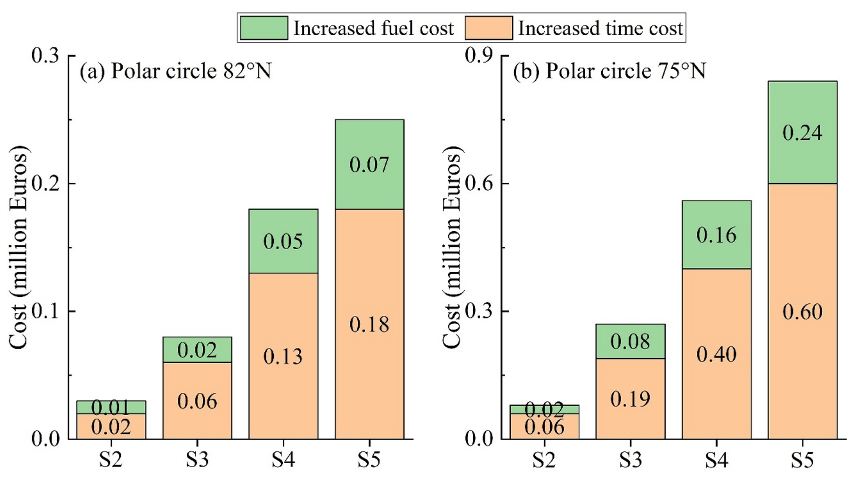

Figure 4. The increased fuel cost and time cost due to flight rerouting at polar circle with latitudes of (a) 82°N and (b) 75°N. The number of affected flights under different scenarios is 3 (flight index: 01–03) under S2, 9 (flight index: 01–09) under S3, 18 (flight index: 01–18) under S4, and 27 (flight index: 01–18 and 01–09) under S5.

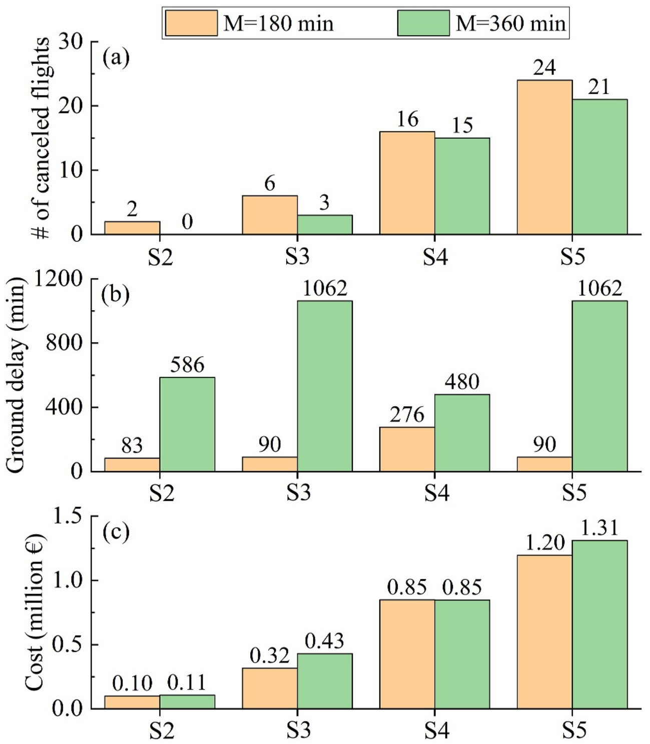

Figure 5. (a) The number of canceled flights and (b) total ground delay time under different scenarios based on the maximum allowable delay time (M) of 180 and 360 min; (c) Economic costs due to flight cancellations and flight delays under different scenarios. The number of affected flights under different scenarios is 3 (flight index: 01–03) under S2, 9 (flight index: 01–09) under S3, 18 (flight index: 01–18) under S4, and 27 (flight index: 01–18 and 01–09) under S5.

results in Table 3, and the increased time costs. It can be seen that under S5, the total economic costs peak at €0.25 million for $\vartheta = 82°$N and €0.84 million for $\vartheta = 75°$N. It clearly shows that rerouting to a smaller latitude of a polar circle increases the costs significantly. Another clear conclusion is that the time cost far exceeds the fuel cost in all scenarios.

5.3. Flight Rescheduling Results

Flight rescheduling is another ATM strategy to address the communication failures poleward of 82°N. To be specific, polar flights are given a ground delay to avoid communication failures north of 82°N. However, some airlines may not accept the initially assigned delay time and would cancel the flights instead in practice. To assess the impact of this response, the maximum allowable delay time (M) is set as 180 min or 360 min. The number of canceled flights and ground delay time for M = 180 min and M = 360 min are illustrated in Figures 5a and 5b, respectively. The number of canceled flights for M = 180 min is larger than that for M = 360 min, whereas the assigned ground delay for M = 180 min is lower than that for M = 360 min.

In contrast to the airborne delay costs associated with airlines, amounting to €74/min, the ground delay cost related to airlines is €16/min (Eurocontrol, 2020). Moreover, it is essential to account for the time cost of passenger delays, and the exact values are detailed in Section 5.2. In addition, the indirect economic costs of flight cancellations for different aircraft types are listed in Table 2. Figure 5c presents the total economic costs, including ground delay costs related to airlines, time delay costs related to passengers, and flight cancellation costs under different scenarios. In general, the overall costs for M = 180 min and M = 360 min are similar in the same simulation scenario. This implies that the choice of M does not have an obvious effect on cost reduction.

5.4. Economic Loss Comparison

Once again, this section reiterates the economic losses across various scenarios to identify the optimal strategy in response to the effects of communication failures on polar flights flying poleward of 82°N. Here are the summarized economic losses for each strategy under simulation scenarios S2, S3, S4, and S5.

1. For flight cancellations:
   (a) Simulation scenario S2: €0.13 million; (b) Simulation scenario S3: €0.44 million; (c) Simulation scenario S4: €0.88 million; (d) Simulation scenario S5: €1.32 million.
2. For flights rerouting along the 82°N:
   (a) Simulation scenario S2: €0.03 million; (b) Simulation scenario S3: €0.08 million; (c) Simulation scenario S4: €0.18 million; (d) Simulation scenario S5: €0.25 million.
3. For flights rerouting along the 75°N:
   (a) Simulation scenario S2: €0.08 million; (b) Simulation scenario S3: €0.27 million; (c) Simulation scenario S4: €0.56 million; (d) Simulation scenario S5: €0.84 million.
4. For flights rescheduling with a maximum allowable delay time of 180 min:
   (a) Simulation scenario S2: €0.10 million; (b) Simulation scenario S3: €0.32 million; (c) Simulation scenario S4: €0.85 million; (d) Simulation scenario S5: €1.20 million.
5. For flights rescheduling with a maximum allowable delay time of 360 min:
   (a) Simulation scenario S2: €0.11 million; (b) Simulation scenario S3: €0.43 million; (c) Simulation scenario S4: €0.85 million; (d) Simulation scenario S5: €1.31 million.

The brief conclusion drawn from this analysis is as follows: flight rerouting demonstrates the least economic losses, followed by flight rescheduling, while flight cancellation incurs the most economic losses.

10.1029/2024SW004136

6. Discussions and Implications

This study examines the critical issue of communication failures poleward of 82°N, including HF communication blackouts and SATCOM failures resulting from space weather events. More importantly, air traffic management solutions are proposed to mitigate the effects on polar air traffic operations. Our findings highlight the severe disruption caused by communication failures, which significantly impair real-time communication between aircraft and ground control, thus increasing operational risks in the challenging polar airspace. Based on a comprehensive analysis, we propose strategies such as flight rescheduling, rerouting, and cancellations as potential solutions to address the challenges posed by space weather.

One of the main implications of this study is the recognition of the need for proactive air traffic management measures to mitigate the impact of communication failures. Flight rescheduling emerges as a viable strategy to optimize polar air traffic operations, allowing airlines to adjust departure times to avoid communication failure periods and minimize disruptions. Similarly, flight rerouting offers an effective approach to circumvent communication failure areas while ensuring continuous air-ground communications. While these strategies require operational adjustments and may pose logistical challenges, they are essential to enhance the safety and reliability of polar flights.

Furthermore, we recognize that flight cancellation is the last resort measure to mitigate the risks associated with communication failures. In situations where alternative communication or navigation system proves inadequate to ensure flight safety, pre-emptive cancellations may be reasonable to avoid exposing passengers and crew to unnecessary risks. While cancellations may incur economic costs and inconvenience for both airlines and passengers, they are crucial for prioritizing safety in polar air traffic management. Overall, the proposed air traffic management solutions offer a comprehensive approach to addressing the challenges posed by communication failures, emphasizing the importance of proactive planning and adaptive strategies in optimizing polar air traffic operations.

7. Conclusions

Due to the limitations of VHF in polar regions, polar flights primarily rely on HF and polar satellite-based SATCOM for reliable coverage and connectivity. HF signals and SATCOM help bridge communication gaps in the polar region. However, space weather events can alter ionospheric conditions, damage satellites, and increase satellite drag. Consequently, HF communications and SATCOM may become impractical or unavailable north of 82°N, leading to operational disruptions for polar flights. Considering the upcoming 25th solar cycle peak in 2025, this study aims to propose air traffic management strategies to mitigate the adverse effects of communication failures, which include flight diversion, flight cancellation, flight rerouting, and flight rescheduling. Based on the daily average of 18 polar flights featuring trajectories crossing the north polar region above 82°N, the simulation results reveal that economic losses tied to these flights can vary from €0.03 million to €1.32 million. This variation is influenced by the duration of the simulated communication failures and the selected air traffic management strategies. Notably, flight rerouting can achieve the minimum economic loss despite additional fuel consumption and flight time. While Air Navigation Service Providers (ANSPs) can contribute to the design of new flight routes, there are instances where this may be hindered by airspace sovereignty issues, particularly during events such as the Russia-Ukraine conflict (Chu et al., 2024). By combining these strategies, the aviation industry can seek to minimize the impact of communication failures north of 82°N and enhance the overall safety and efficiency of air travel over polar regions. In the long term, mega constellations have the potential to offer improved global coverage and redundancy for aviation communication, especially in remote regions (Lagunas et al., 2024; Ravishankar et al., 2021). However, during extreme space weather events, ionospheric disturbances can still degrade signals or disrupt multiple satellites, limiting their reliability. While these networks represent a major advancement, their resilience to space weather remains a key challenge requiring further research.

In addition to communication failures, space weather can also hinder normal flight operations by degrading GNSS performance (Nie et al., 2022; Zhao et al., 2022) and increasing cosmic radiation (Chen et al., 2023; Hands et al., 2022). The failure of satellite navigation can have a wide range of effects on flight operations, impacting safety, efficiency, and the overall reliability of air travel (Enge et al., 2015). Higher cosmic radiation exposure may contribute to a higher risk of health issues, including an elevated risk of cancer (Ali et al., 2020). For this reason, Aviation authorities have established occupational exposure limits for aircrews to minimize the risks

10.1029/2024SW004136

associated with cosmic radiation (Bagshaw, 2008). In summary, studying space weather is essential for maintaining the safety, reliability, and efficiency of aviation operations. It enables the development of proactive measures, contingency plans, and regulatory frameworks to address the challenges posed by space weather events.

Appendix A

According to the Base of Aircraft Data (BADA) (Eurocontrol, 2022), the nominal fuel flow f (kg/min) for jet engine aircraft can be calculated by a function of thrust specific fuel consumption η (kg/(min·kN)) and engine thrust Thr (N).

$$f = \frac{\eta \cdot Thr}{1000} \tag{A1}$$

where η is associated with the thrust-specific fuel consumption coefficients C_{f_1}, C_{f_2}, and true airspeed (TAS) v (km/h).

$$\eta = C_{f_1}\left(1 + \frac{v}{1.852 \cdot C_{f_2}}\right) \tag{A2}$$

During the cruise phase, it is assumed that drag force D (N) is equal to the thrust in (A3), and the method for calculating drag force is listed in Equations A4–A6.

$$Thr = D \tag{A3}$$

$$D = \frac{1}{2} C_D \cdot \rho \cdot \left(\frac{v}{3.6}\right)^2 \cdot S \tag{A4}$$

$$C_D = C_{D_0.CR} + C_{D_2.CR} \cdot (C_L)^2 \tag{A5}$$

$$C_L = \frac{2 \cdot m \cdot g_0}{\rho \cdot \left(\frac{v}{3.6}\right)^2 \cdot S \cdot \cos\theta} \tag{A6}$$

where C_D represents the standard drag coefficient, ρ denotes the standard air density (kg/m^3), and S stands for the wing reference area (m^2). Additionally, $C_{D_0.CR}$ and $C_{D_2.CR}$ represent drag coefficients. The lift coefficient C_L is associated with aircraft mass (m) and bank angle θ.

The wind speed $\boldsymbol{w}$ holds significance in determining flight time, thereby impacting fuel consumption. The ground speed vector $\boldsymbol{g}$ can be expressed as $\boldsymbol{g} = \boldsymbol{w} + \boldsymbol{v}$. Consequently, the ground speed (in km/h) can be expressed by $g = |\boldsymbol{w} + \boldsymbol{v}|$. Hence, it will take the time of L/g to flight a particular flight distance L (in km), and the fuel consumption F (in kg) can be calculated by:

$$F = 60 \times f \times \frac{L}{g} \tag{A7}$$

Conflict of Interest

The authors declare no conflicts of interest relevant to this study.

Data Availability Statement

The polar flight data are publicly accessible at https://opensky-network.org/.

Acknowledgments

This work was supported by the Hong Kong Research Grants Council (RGC) projects (RGC/Gov No. PolyU 15221620/B-Q80Q and RGC/Gov No. PolyU 15205821/B-Q84W), the Stable Support Plan Program of Shenzhen Natural Science Fund (Grant 20200925153644003), and Shenzhen Science and Technology Program (Grant JCYJ20220530113402004).

References

Airlines for America. (2023). U.S. Passenger carrier delay costs. Retrieved from https://www.airlines.org/dataset/u-s-passenger-carrier-delay-costs/#:~:text=In%202022%2C%20the%20average%20cost,percent%20to%20%2442.15%20per%20minute

Albers, S., & Rundshagen, V. (2020). European airlines' strategic responses to the COVID-19 pandemic (January-May, 2020). *Journal of Air Transport Management*, *87*, 101863. https://doi.org/10.1016/j.jairtraman.2020.101863

Albright, J. (2020). High latitude operations. https://code7700.com/high_latitude.htm

Alharasees, O., Jazzar, A., Kale, U., & Rohacs, D. (2023). Aviation communication: The effect of critical factors on the rate of misunderstandings. *Aircraft Engineering & Aerospace Technology*, *95*(3), 379–388. https://doi.org/10.1108/AEAT-02-2022-0052

Ali, Y. F., Cucinotta, F. A., Ning-Ang, L., & Zhou, G. (2020). Cancer risk of low dose ionizing radiation. *Frontiers in Physics*, *8*, 234. https://doi.org/10.3389/fphy.2020.00234

Anderson, B. J., Angappan, R., Barik, A., Vines, S. K., Stanley, S., Bernasconi, P. N., et al. (2021). Iridium communications satellite constellation data for study of Earth's magnetic field. *Geochemistry, Geophysics, Geosystems*, *22*(8), e2020GC009515. https://doi.org/10.1029/2020GC009515

Bagshaw, M. (2008). Cosmic radiation in commercial aviation. *Travel Medicine and Infectious Disease*, *6*(3), 125–127. https://doi.org/10.1016/j.tmaid.2007.10.003

Bain, H., Copeland, K., Onsager, T., & Steenburgh, R. (2023). NOAA space weather prediction center radiation advisories for the international civil aviation organization. *Space Weather*, *21*(7), e2022SW003346. https://doi.org/10.1029/2022SW003346

Bureau of Meteorology. (2023). Aviation services - space weather advisories. Retrieved from http://www.bom.gov.au/aviation/data/education/space-weather-advisories.pdf

Bust, G. S., Liles, W., & Mitchell, C. (2021). *Space weather influences on HF, UHF, and VHF radio propagation* (pp. 153–163). Space Weather Effects and Applications. https://doi.org/10.1002/9781119815570.ch7

Caspi, A., Barthelemy, M., Bussy-Virat, C., Cohen, I., DeForest, C., Jackson, D., et al. (2022). Small satellite mission concepts for space weather research and as pathfinders for operations. *Space Weather*, *20*(2), e2020SW002554. https://doi.org/10.1029/2020SW002554

Chang, Y. (2020). An enhanced rerouting cost estimation algorithm towards internet of drone. *The Journal of Supercomputing*, *76*(12), 10036–10049. https://doi.org/10.1007/s11227-020-03243-9

Chen, Q., Giambene, G., Yang, L., Fan, C., & Chen, X. (2021). Analysis of inter-satellite link paths for LEO mega-constellation networks. *IEEE Transactions on Vehicular Technology*, *70*(3), 2743–2755. https://doi.org/10.1109/TVT.2021.3058126

Chen, X., Xu, S., Song, X., Huo, R., & Luo, X. (2023). Astronaut radiation dose calculation with a new galactic cosmic ray model and the AMS-02 data. *Space Weather*, *21*(4), e2022SW003285. https://doi.org/10.1029/2022SW003285

Chen, Z., Liao, W., Li, H., Wang, J., Deng, X., & Hong, S. (2022). Prediction of global ionospheric TEC based on deep learning. *Space Weather*, *20*(4), e2021SW002854. https://doi.org/10.1029/2021SW002854

Chu, C., Zhang, H., Zhang, J., Cong, L., & Lu, F. (2024). Assessing impacts of the Russia-Ukraine conflict on global air transportation: From the view of mass flight trajectories. *Journal of Air Transport Management*, *115*, 102522. https://doi.org/10.1016/j.jairtraman.2023.102522

Darnel, J. M., Seaton, D. B., Bethge, C., Rachmeler, L., Jarvis, A., Hill, S. M., et al. (2022). The GOES-R solar UltraViolet imager. *Space Weather*, *20*(4), e2022SW003044. https://doi.org/10.1029/2022SW003044

Di Vaio, A., & Varriale, L. (2020). Blockchain technology in supply chain management for sustainable performance: Evidence from the airport industry. *International Journal of Information Management*, *52*, 102014. https://doi.org/10.1016/j.ijinfomgt.2019.09.010

Dobrijevic, D. (2022). Solar flares: What are they and how do they affect Earth? https://www.space.com/solar-flares-effects-classification-formation

Echer, E., Gonzalez, W. D., Tsurutani, B. T., & Gonzalez, A. L. C. d. (2008). Interplanetary conditions causing intense geomagnetic storms (Dst≤− 100 nT) during solar cycle 23 (1996–2006). *Journal of Geophysical Research*, *113*(A5). https://doi.org/10.1029/2007JA012744

Enge, P., Enge, N., Walter, T., & Eldredge, L. (2015). Aviation benefits from satellite navigation. *New Space*, *3*(1), 19–35. https://doi.org/10.1089/space.2014.0011

Eurocontrol. (2020). Standard inputs for economic analyses. Retrieved from https://www.eurocontrol.int/publication/eurocontrol-standard-inputs-economic-analyses

Eurocontrol. (2022). User manual for the Base of aircraft data (BADA) revision 3.16. Retrieved from https://www.eurocontrol.int/model/bada

FAA. (2022). Polor route operations. Retrieved from https://www.faa.gov/sites/faa.gov/files/2022-11/Polar_Route_Operations.pdf

Fiori, R. A., Kumar, V. V., Boteler, D. H., & Terkildsen, M. B. (2022). Occurrence rate and duration of space weather impacts on high-frequency radio communication used by aviation. *Journal of Space Weather and Space Climate*, *12*, 21. https://doi.org/10.1051/swsc/2022017

Goodman, J. M. (2005). Operational communication systems and relationships to the ionosphere and space weather. *Advances in Space Research*, *36*(12), 2241–2252. https://doi.org/10.1016/j.asr.2003.05.063

Hands, A., Lei, F., Davis, C., Clewer, B., Dyer, C., & Ryden, K. (2022). A new model for nowcasting the aviation radiation environment with comparisons to in situ measurements during gles. *Space Weather*, *20*(8), e2022SW003155. https://doi.org/10.1029/2022SW003155

Hapgood, M. (2022). Ionospheric science: An example of the importance of diversity in approaches to scientific research. *Atmosphere*, *13*(3), 394. https://doi.org/10.3390/atmos13030394

Hapgood, M., Angling, M. J., Attrill, G., Bisi, M., Cannon, P. S., Dyer, C., et al. (2021). Development of space weather reasonable worst-case scenarios for the UK national risk assessment. *Space Weather*, *19*(4). https://doi.org/10.1029/2020SW002593

Hapgood, M., Liu, H., & Lugaz, N. (2022). SpaceX-Sailing close to the space weather? *Space Weather*, *20*(3), e2022SW003074. https://doi.org/10.1029/2022SW003074

Horne, R., Glauert, S., Meredith, N., Boscher, D., Maget, V., Heynderickx, D., & Pitchford, D. (2013). Space weather impacts on satellites and forecasting the Earth's electron radiation belts with SPACECAST. *Space Weather*, *11*(4), 169–186. https://doi.org/10.1002/swe.20023

Hu, Y., Xu, B., Bard, J. F., Chi, H., & Gao, M. (2015). Optimization of multi-fleet aircraft routing considering passenger transiting under airline disruption. *Computers and Industrial Engineering*, *80*, 132–144. https://doi.org/10.1016/j.cie.2014.11.026

IATA. (2024). Jet fuel price monitor. Retrieved from https://www.iata.org/en/publications/economics/fuel-monitor/

ICAO. (2008). *Manual on air traffic management system requirements*, International Civil Aviation Organization. Retrieved from https://www.icao.int/airnavigation/IMP/Documents/Doc%209882%20-%20Manual%20on%20ATM%20Requirements.pdf

Kauristie, K., Andries, J., Beck, P., Berdermann, J., Berghmans, D., Cesaroni, C., et al. (2021). Space weather services for civil aviation—Challenges and solutions. *Remote Sensing*, *13*(18), 3685. https://doi.org/10.3390/rs13183685

Kay, C., Mays, M. L., & Collado-Vega, Y. M. (2022). Osprei: A coupled approach to modeling CME-driven space weather with automatically generated, user-friendly outputs. *Space Weather*, *20*(4), e2021SW002914. https://doi.org/10.1029/2021SW002914

Kleimenova, N., Gromova, L., Gromov, S., & Malysheva, L. (2021). High-latitude geomagnetic disturbances and field aligned currents in the recovery phase of the large magnetic storm on June 21–26, 2015. *Geomagnetism and Aeronomy*, *61*(4), 520–530. https://doi.org/10.1134/S0016793221040071

Knipp, D. J., Ramsay, A., Beard, E., Boright, A., Cade, W., Hewins, I., et al. (2016). The May 1967 great storm and radio disruption event: Extreme space weather and extraordinary responses. *Space Weather*, *14*(9), 614–633. https://doi.org/10.1002/2016SW001423

Kruglyakov, M., Kuvshinov, A., & Marshalko, E. (2022). Real-time 3-D modeling of the ground electric field due to space weather events. A concept and its validation. *Space Weather*, *20*(4), e2021SW002906. https://doi.org/10.1029/2021SW002906

Lagunas, E., Chatzinotas, S., & Ottersten, B. (2024). Low-Earth orbit satellite constellations for global communication network connectivity. *Nature Reviews Electrical Engineering*, *1*, 1–10. https://doi.org/10.1038/s44287-024-00088-9

Li, T., Jin, J., Li, W., Ren, Z., & Kuang, L. (2021). Research on interference avoidance effect of OneWeb satellite constellation's progressive pitch strategy. *International Journal of Satellite Communications and Networking*, *39*(5), 524–538. https://doi.org/10.1002/sat.1399

Lin, C. J., Lin, P.-H., Chen, H.-J., Hsieh, M.-C., Yu, H.-C., Wang, E. M.-Y., & Ho, H. L. (2012). Effects of controller-pilot communication medium, flight phase and the role in the cockpit on pilots' workload and situation awareness. *Safety Science*, *50*(9), 1722–1731. https://doi.org/10.1016/j.ssci.2012.04.007

Long, J., & Zhang, T. (2024). Pillars of space traffic management in the era of LEO mega-constellations: A global perspective. *Advances in Space Research*, *74*(2), 800–816. https://doi.org/10.1016/j.asr.2024.04.011

Ma, T., Qian, B., Wang, Y., Liu, X., & Zhou, H. (2023). Airborne internet: An ultradense LEO networks empowered satellite-to-aircraft access and resource management approach. *IEEE Internet of Things Journal*, *10*(23), 20241–20253. https://doi.org/10.1109/JIOT.2023.3281404

Malandri, C., Mantecchini, L., Paganelli, F., & Postorino, M. N. (2020). Impacts of unplanned aircraft diversions on airport ground operations. *Transportation Research Procedia*, *47*, 537–544. https://doi.org/10.1016/j.trpro.2020.03.129

McDowell, J. C. (2020). The low earth orbit satellite population and impacts of the SpaceX Starlink constellation. *The Astrophysical Journal Letters*, *892*(2), L36. https://doi.org/10.3847/2041-8213/ab8016

Merkert, R., & Webber, T. (2018). How to manage seasonality in service industries–the case of price and seat factor management in airlines. *Journal of Air Transport Management*, *72*, 39–46. https://doi.org/10.1016/j.jairtraman.2018.07.005

NAV CANADA. (2017). Polar routes - Past, present and future. Retrieved from https://www.navcanada.ca/en/news/blog/polar-routes–past-present-and-future.aspx#:~:text=Air%20traffic%20operating%20on%20polar,greenhouse%20gas%20emission%20reductions%20annually

Nie, W., Rovira-Garcia, A., Li, M., Fang, Z., Wang, Y., Zheng, D., & Xu, T. (2022). The mechanism for GNSS-based kinematic positioning degradation at high-latitudes under the March 2015 great storm. *Space Weather*, *20*(6), e2022SW003132. https://doi.org/10.1029/2022SW003132

Okoh, D., Seemala, G., Rabiu, A., Uwamahoro, J., Habarulema, J., & Aggarwal, M. (2018). A Hybrid Regression-Neural Network (HR-NN) method for forecasting the solar activity. *Space Weather*, *16*(9), 1424–1436. https://doi.org/10.1029/2018SW001907

Oliveira, D. M., & Zesta, E. (2019). Satellite orbital drag during magnetic storms. *Space Weather*, *17*(11), 1510–1533. https://doi.org/10.1029/2019SW002287

Palmerio, E., Lee, C. O., Mays, M. L., Luhmann, J. G., Lario, D., Sánchez-Cano, B., et al. (2022). CMEs and SEPs during November–December 2020: A challenge for real-time space weather forecasting. *Space Weather*, *20*(5), e2021SW002993. https://doi.org/10.1029/2021SW002993

Pinkerton, A. (2019). *Radio: Making waves in sound*. Reaktion Books.

Portella, I. P., de O Moraes, A., da Silva Pinho, M., Sousasantos, J., & Rodrigues, F. (2021). Examining the tolerance of GNSS receiver phase tracking loop under the effects of severe ionospheric scintillation conditions based on its bandwidth. *Radio Science*, *56*(6), 1–11. https://doi.org/10.1029/2020RS007160

Ravishankar, C., Gopal, R., BenAmmar, N., Zakaria, G., & Huang, X. (2021). Next-generation global satellite system with mega-constellations. *International Journal of Satellite Communications and Networking*, *39*(1), 6–28. https://doi.org/10.1002/sat.1351

Ruck, J. J., & Themens, D. R. (2021). Impacts of auroral precipitation on HF propagation: A hypothetical over-the-horizon radar case study. *Space Weather*, *19*(12), e2021SW002901. https://doi.org/10.1029/2021SW002901

Singh, A., Siingh, D., & Singh, R. (2010). Space weather: Physics, effects and predictability. *Surveys in Geophysics*, *31*(6), 581–638. https://doi.org/10.1007/s10712-010-9103-1

Singh, A. K., Bhargawa, A., Siingh, D., & Singh, R. P. (2021). Physics of space weather phenomena: A review. *Geosciences*, *11*(7), 286. https://doi.org/10.3390/geosciences11070286

Smith, M., Moser, D., Strohmeier, M., Lenders, V., & Martinovic, I. (2018). Undermining privacy in the aircraft communications addressing and reporting system (ACARS). *Proceedings on Privacy Enhancing Technologies*, *2018*(3), 105–122. https://doi.org/10.3929/ethz-b-000294042

Song, X., Yang, R., & Zhan, X. (2020). An analysis of global ionospheric disturbances and scintillations during the strong magnetic storm in September 2017. *Aerospace Systems*, *3*(4), 255–263. https://doi.org/10.1007/s42401-020-00067-6

Tooley, M., & Wyatt, D. (2017). *Aircraft communications and navigation systems*. Routledge. https://doi.org/10.1201/9781315858982

Tsurutani, B., Judge, D., Guarnieri, F., Gangopadhyay, P., Jones, A., Nuttall, J., et al. (2005). The October 28, 2003 extreme EUV solar flare and resultant extreme ionospheric effects: Comparison to other Halloween events and the Bastille Day event. *Geophysical Research Letters*, *32*(3). https://doi.org/10.1029/2004GL021475

Tsurutani, B., Verkhoglyadova, O., Mannucci, A., Lakhina, G., Li, G., & Zank, G. (2009). A brief review of "solar flare effects" on the ionosphere. *Radio Science*, *44*(01), 1–14. https://doi.org/10.1029/2008rs004029

Tsurutani, B. T., Zank, G. P., Sterken, V. J., Shibata, K., Nagai, T., Mannucci, A. J., et al. (2022). Space plasma physics: A review. *IEEE Transactions on Plasma Science*, *51*(7), 1595–1655. https://doi.org/10.1109/TPS.2022.3208906

U.S. Department of Transportation. (2022). Flight delays and cancellations. Retrieved from https://www.transportation.gov/individuals/aviation-consumer-protection/flight-delays-cancellations#:~:text=Some%20problems%2C%20like%20bad%20weather,flights%20are%20delayed%20or%20cancelled

Wang, J., Xiao, F., Dobruszkes, F., & Wang, W. (2023). Seasonality of flights in China: Spatial heterogeneity and its determinants. *Journal of Air Transport Management*, *108*, 102354. https://doi.org/10.1016/j.jairtraman.2022.102354

Xue, D., Hsu, L.-T., Wu, C.-L., Lee, C.-H., & Ng, K. K. (2021). Cooperative surveillance systems and digital-technology enabler for a real-time standard terminal arrival schedule displacement. *Advanced Engineering Informatics*, *50*, 101402. https://doi.org/10.1016/j.aei.2021.101402

Xue, D., Ng, K. K., & Hsu, L.-T. (2020). Multi-objective flight altitude decision considering contrails, fuel consumption and flight time. *Sustainability*, *12*(15), 6253. https://doi.org/10.3390/su12156253

Xue, D., Yang, J., & Liu, Z. (2022). Potential impact of GNSS positioning errors on the satellite-navigation-based air traffic management. *Space Weather*, *20*(7), e2022SW003144. https://doi.org/10.1029/2022SW003144

Xue, D., Yang, J., Liu, Z., & Cong, W. (2023). Forward-looking study of solar maximum impact in 2025: Effects of satellite navigation failure on aviation network operation in the greater bay area, China. *Space Weather*, *21*(12), e2023SW003678. https://doi.org/10.1029/2023SW003678

Xue, D., Yang, J., Liu, Z., & Wang, B. (2022b). An optimized solution to long-distance flight routes under extreme cosmic radiation. *Space Weather*, *20*(12), e2022SW003264. https://doi.org/10.1029/2022SW003264

Xue, D., Yang, J., Liu, Z., & Yu, S. (2023). Examining the economic costs of the 2003 Halloween storm effects on the North Hemisphere aviation using flight data in 2019. *Space Weather*, *21*(3), e2022SW003381. https://doi.org/10.1029/2022SW003381

Yimga, J., & Gorjidooz, J. (2019). Airline schedule padding and consumer choice behavior. *Journal of Air Transport Management*, *78*, 71–79. https://doi.org/10.1016/j.jairtraman.2019.05.001

Zhang, J., Cai, Y., Xue, C., Xue, Z., & Cai, H. (2022). LEO mega constellations: Review of development, impact, surveillance, and governance. *Space: Science and Technology*, *2022*. https://doi.org/10.34133/2022/9865174

Zhao, D., Li, W., Li, C., Tang, X., Wang, Q., Hancock, C. M., et al. (2022). Ionospheric phase scintillation index estimation based on 1 Hz geodetic GNSS receiver measurements by using continuous wavelet transform. *Space Weather*, *20*(4), e2021SW003015. https://doi.org/10.1029/2021SW003015

Zinke, L. (2023). Halloween-like solar storm impacts. *Nature Reviews Earth and Environment*, *4*(11), 1. https://doi.org/10.1038/s43017-023-00496-9